

Microstructure, Mechanical Properties and Machinability Studies of Al7075/SiC/h-BN Hybrid Nanocomposite Fabricated via Ultrasonic-assisted Squeeze Casting

Sourabh Kumar Soni

Research Scholar
Vellore Institute of Technology
School of Mechanical Engineering
Vellore
India

Benedict Thomas

Associate Professor
Vellore Institute of Technology
School of Mechanical Engineering
Vellore
India

The present research article deals with the microstructure, mechanical properties and machinability investigation of squeeze-cast Al7075 and Al7075/SiC/h-BN hybrid nanocomposite. The Al7075 alloy nanocomposite has been reinforced by micro-size SiC (1 wt.%) particles and h-BN (0.5 wt.%) nanoparticles, prepared via ultrasonic-assisted melt-stirring approach. In order to achieve the better mixing of reinforcements, diminish the agglomeration effect of nanoparticles and improved wettability of the particles in the melt, SiC and h-BN powders have been ball-milled for the duration of 4 h. The microstructural investigation of the prepared nanocomposite was carried out by using optical microscopy (OM), scanning electron microscopy (SEM) and x-ray mapping analysis. The x-ray mapping and optical microscopic analysis show good dispersion uniformity of reinforcements and refinement in the grain sizes. The investigation of mechanical properties of hybrid nanocomposite shows the significant improvement of about 35.33 %, 21.69 %, 13.87 % and 12.27 % in the offset yield strength, ultimate tensile strength, Rockwell hardness and microhardness (Vickers), respectively. Furthermore, the machinability analysis has been performed to examine the influence of several machining parameters such as cutting speed, feed rate and depth of cut on the surface roughness, cutting force and chips length of the squeeze-cast hybrid nanocomposites under dry and minimum quantity lubrication (MQL) machining conditions. The outcomes of the machinability analysis for hybrid nanocomposites are compared with the Al7075 specimen and discussed.

Keywords: Hybrid Nanocomposite, Ultrasonic-assisted Squeeze Casting, Mechanical Properties, Machinability, Roughness.

1. INTRODUCTION

Aluminium and its alloy are widely preferred over the conventional materials in automotive, sports goods, marine and aircraft industries owing to its superior properties such as low density, good strength to weight ratio and wear resistance [1,2]. Literature demonstrated substantial augmentation in the mechanical properties and resistance to wear of the aluminium based materials upon reinforcing micro and nano-sized reinforcements such as silicon carbide (SiC) [3], titanium oxide (TiO₂) [4], alumina (Al₂O₃) [5,6], graphene (GNPs) [7], titanium boride (TiB₂) [8], B₄C [9] and carbon nanotubes (CNTs) [10]. The above-stated aluminium based material reinforced with micro and nano-size reinforcements (AMMCs) are widely used as automobile bodies, aircraft structure, cylinder liners, pistons, bearing surfaces, gears, brake components and connecting rods [1].

To fabricate AMMCs, the earlier researchers frequently employed numerous processing techniques such as powder metallurgy [11], compocasting [8], pressure infiltration, casting (stir and squeeze) [10–12] and friction stir processing [1]. Among the other, the casting route is widely preferred as a particularly promising synthesis method due to the ease of processing, higher production rate and cost-effectiveness in producing products used in various engineering applications [1]. In order to attain the homogenous mixing and dispersion uniformity of reinforcements in the melt during the casting approach, the mechanical-stirring approach was used, which is not an effective technique to fabricate AMMCs with micro and nano-size reinforcements owing to the formation of particle agglomeration and poor wettability. In previous literature, numerous researchers adopted a reinforcement pre-processing (pre-dispersion) route [12,13] and ultrasonic-assisted casting approach [14] to reduce the chance of particle agglomeration as well as uniform mixing of reinforcements in the matrix.

Over the past decade, Al-based materials reinforced with hard ceramic particle (SiC) are increasingly being used in automotive components such as brake pads, connecting rods, pistons, driveshaft and disc brakes [1],

Received: January 2020, Accepted: March 2020

Correspondence to: Dr. Benedict Thomas
School of Mechanical Engineering,
Vellore Institute of Technology, Vellore, 632014, India.
E-mail: benedict.thomas@vit.ac.in

doi: 10.5937/fme2003532K

© Faculty of Mechanical Engineering, Belgrade. All rights reserved

FME Transactions (2020) 48, 532-542 532

[15]. The addition of SiC particles in Al alloy improves the resistance to wear and mechanical properties of the resulting composites [11]. In previous literature, hexagonal boron nitride (h-BN) has been used as a secondary reinforcement in the preparation of Al-based hybrid nanocomposites as it acts as a solid lubricant and increases the self-lubricating nature and toughness of the resulting composites. Previous research publications showed that the mechanical, machinability and tribological characteristics could be enhanced with the reinforcement of h-BN nanoparticles in the matrix [12,16].

High precision components require an advanced machining operation that offers close dimensional tolerances and smooth surface finish. It is well known that an increase in surface roughness (SR) leads to higher friction. The reliability and life cycle of the components that are prepared of composites are strongly affected by their surface quality, which can withstand corrosion, temperature and stress. The reinforcement of hard SiC particles in the base matrix often adds intricacy in the machining operation of resulting composites [17]. These complexities in the machining of composites confine their variety of commercial applications.

The machinability of composites primarily depends on numerous parameters such as type of machine, cutting tool, machining process parameters, reinforcement type, weight % of reinforcement, size of the reinforcing particles, distribution of reinforcements, cutting fluid and type of coolant [12,15,16,18,19]. Nearly one-fourth of the total machining cost is accompanying the machining tool, and one-fifth machine downtime happens owing to the failure of the cutting tool [18]. Moreover, in specific applications, the cost of cutting fluid is around 20% of the total cost of machining [16]. Conventional cutting tools cannot sustain machining of composites and outcomes in greater SR and high rate of tool wear, whereas costly PCD inserts may result in a higher cost of manufacturing. In order to address above-stated difficulties, researchers are searching alternatives such as appropriate cutting tool materials, additional reinforcement of solid-lubricant particles in composites, advanced cutting techniques and optimum machining conditions for machining processes.

Despite numerous investigations on the machinability of AMMCs, the literature on the machining of ultrasonic-assisted squeeze-cast Al7075/SiC/h-BN hybrid nanocomposite under dry and minimum quantity lubrication (MQL) machining environment is seldom found. The present experimental investigation is performed to examine the microstructure, mechanical properties and machinability studies of the Al7075/SiC/h-BN hybrid nanocomposite produced via the combined method of reinforcement pre-dispersion and ultrasonic-assisted squeeze casting. The machinability studies have been conducted to examine the influence of several machining parameters including depth of cut (0.5 mm), cutting speed (180 and 200 m/min) and feed rate (0.1, 0.2, and 0.3 mm/rev) on the cutting force, surface roughness and chips formation of the squeeze-cast Al7075/SiC/h-BN hybrid nanocomposites under dry and MQL turning conditions.

2. MATERIALS AND METHODS

In this work, Al7075 alloy was used as the matrix phase owing to its wide-ranging applications in automobile and aircraft components. The chemical composition of the Al7075 alloy was Mg (2.42), Si (0.13), Mn (0.12), Cu (1.42), Fe (0.42), Ti (0.11), Zn (5.4), Cr (0.21), and Al (Balance). Micron-size (SiC) and nano-size (h-BN) particles were used as the reinforcing material. Morphology and particle size of the as-received reinforcing particles (SiC and h-BN) are presented in figures 1 (a-b).

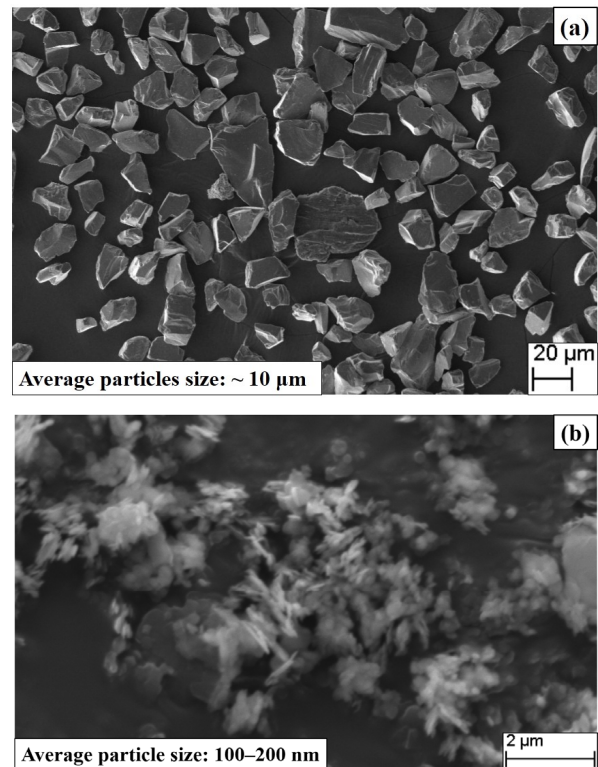


Figure 1. Morphologies of as-received (a) SiC and (b) nano h-BN particles.

2.1 Al7075-based HNC fabrication process

It has already been discussed that the mechanical stirrer used in the casting is not much efficient method for achieving the dispersion uniformity of reinforcing particles in the matrix. Therefore, in this study, the combined approach of ultrasonic-assisted casting and pre-dispersion (pre-processing) of reinforcements has been adopted.

2.2 Pre-processing of reinforcements

Harsh agglomeration of h-BN nanoparticles is evident in the SEM image (figure 1b). Hence, prior to the preparation of Al7075 based HNC, pre-dispersion of SiC/h-BN particles is mandatory to achieve the homogenous mixing and dispersion uniformity. In this study, the low-speed ball milling route was adopted to pre-disperse the reinforcements. The measured amount of SiC and MWCNTs powders were ball-milled employing ball mill set-up at a rotational speed of 200 rpm for 4 hours. The ball to powder weight ratio (BPR) was kept at 10:1.

2.3 Ultrasonic-assisted melt stirring process

Al7075 based MMCs reinforced with 1 wt.% of micron-size SiC particles and 0.5 wt.% of nano h-BN particles were prepared through the ultrasonic-assisted squeeze casting approach. Squeeze casting facility (SWAMEQIP made) equipped with a bottom pouring mechanism was employed for the preparation of the unreinforced Al7075 and HNC specimens. To accomplish the better dispersion of reinforcing particles in the melt, the mechanical stirrer and ultrasonic probe was used in the present investigation. The photographic view of the ultrasonic-assisted melt stirring set-up is presented in figure 3.



Figure 2. Fabricated squeeze-cast specimens after skinning.

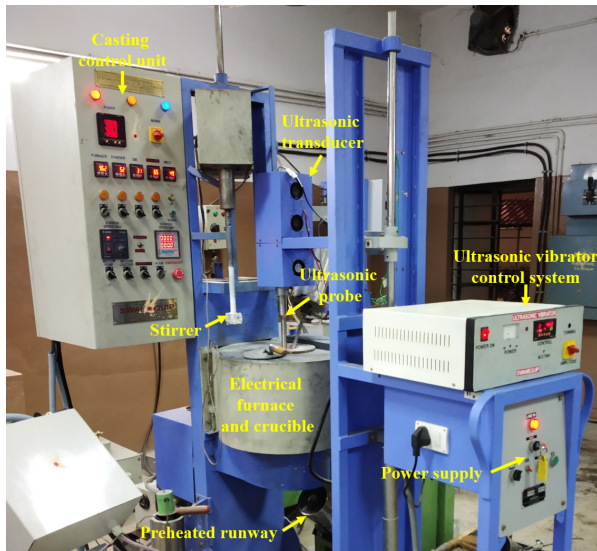


Figure 3. A photographic view of ultrasonic-assisted melt stirring set-up

The unit consists of a furnace, reinforcement preheating chamber, ultrasonic transducer, bottom pouring mechanism, mechanical stirrer, preheated runway and hydraulic press. At first, the measured quantity of preheated Al7075 alloy in the form of small blocks was placed into graphite coated crucible and melted to 850°C in an electric resistance heating furnace. For the preparation of HNC, an adequate quantity of pre-processed (ball-milled) SiC/h-BN powder mixture was placed into the reinforcement pre-heating chamber and preheated up to a temperature of 300 °C for the duration of 4 h. Furthermore, when the Al7075 alloy was reached in the molten state, the vortex on the melt was generated

by using a mechanical stirrer. Later, the pre-heated SiC/h-BN powder mixture was appended into the melted slurry through a reinforcement injector and stirred at 550 rpm for 10 min. When the stirring process was completed, the mechanical stirrer was replaced with ultrasonic vibrator and, ultrasonication was performed for 3 minutes to break the agglomerates of reinforcements and achieve the dispersion uniformity. Lastly, the bottom gateway of the furnace was opened, and HNC slurry was poured into a cylindrical die with a squeezing pressure of 101 MPa. Through this process, the squeeze-cast Al7075 and Al7075/SiC/h-BN HNC specimens were prepared (shown in figure 2). The schematic of the methodology and squeeze casting set-up used for the preparation of Al7075 and HNC samples is presented in figure 4.

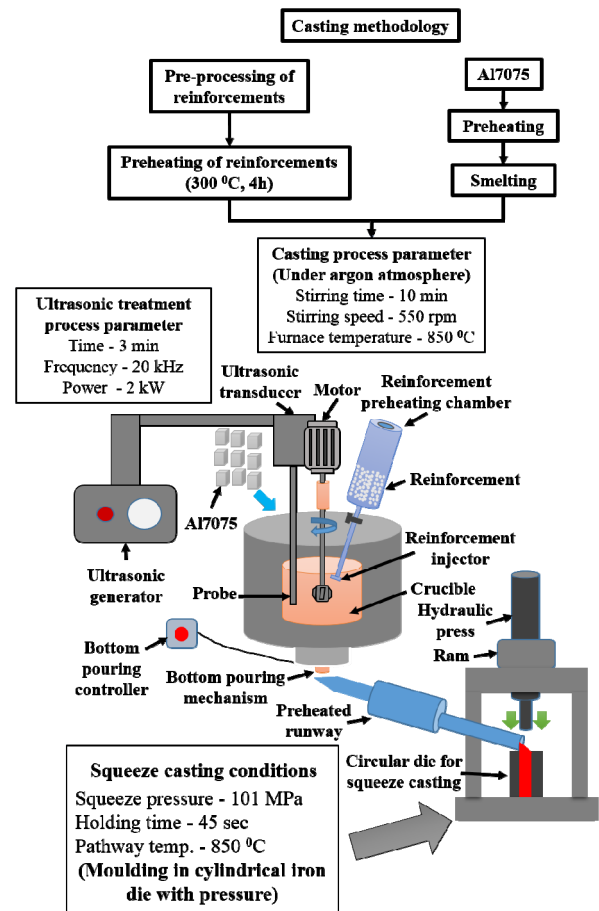


Figure 4. Schematic of the methodology adopted for the preparation of specimens.

2.4 Material characterization

The microstructure of as-received reinforcement particles and 4 h ball-milled SiC/h-BN powders was examined using SEM (EVO 18, ZEISS) fitted with energy dispersive spectroscopy (EDS). The investigation of mechanical properties such as tensile strength, hardness, microhardness and microstructural examination were performed on the prepared Al7075 and Al7075/SiC/h-BN HNC specimens. The ultimate tensile strength (UTS) and yield strength (YS) of the prepared specimens were evaluated using a computerized tensile testing machine (INSTRON 4000) according to the ASTM E08-8 standards. Three polished specimens were tested for each composition, and the average value of

UTS and YS was reported as the final tensile properties. The hardness and microhardness of the prepared specimens were measured in a Rockwell hardness tester (100 kgf load, 1/16" ball indenter, 10 s dwell time) and Vickers micro-hardness tester (500 g load, 30 s dwell time), respectively. The hardness tests were carried out at five (Rockwell) and twenty (Vickers) random locations on the polished surface of the specimens, and average values were considered as a final reading. In order to examine the grain structure of the squeeze-cast Al7075 and HNC, specimens were prepared using the standard metallographic methodology and etched with Keller's reagent. Furthermore, the Zeiss Axio optical microscope was used to examine the etched specimens. The presence and dispersal of reinforcements in the HNC were analyzed through SEM equipped with EDS and elemental mapping analysis. Lastly, the fractured surface of the HNC was examined using SEM.

The high-speed Turn 5075 SPM CNC turning machine was used to analyze the effect of machining parameters for instance FR (0.1, 0.2 and 0.3 mm/rev), CS (180 and 200 m/min) and DOC (0.5 mm) on the cutting force, SR and chips formation under dry and MQL machining environments. The above-mentioned turning process parameter and machining environments are chosen deliberately, and machining experiments were conducted in an ambient environment. The geometrical details and photographic image of the tungsten carbide cutting insert used in the machining of squeeze-cast specimens are shown in figure 5. In order to minimize the errors, every turning operation was reiterated three times.

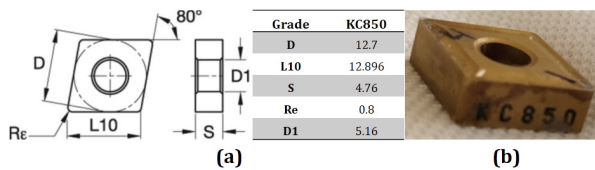


Figure 5 Geometry and photographic image of the tungsten carbide cutting insert.

The cutting forces during the turning operation was measured through the piezoelectric dynamometer. After completion of each run, the SR of the machined surface was assessed through the surface profilometer (MAHR, Germany). The measurement of SR was performed at six different locations on the machined surface of the squeeze-cast Al7075 and HNC specimens. The average value of the six readings was calculated and taken as a final reading. Later, the variation in the chip length was analyzed via photographic images. The technical specifications of the surface profilometer and CNC machine used in the present investigation have been described elsewhere [12].

3. RESULTS AND DISCUSSION

3.1 Microstructure investigation of 4 h ball-milled SiC/h-BN powders

Figure 6 shows the SEM image and EDS analysis of SiC/h-BN powders dispersed through ball milling for a duration of 4 h. From this low-magnification SEM image, it can be observed that due to 4 h ball milling, the SiC and h-BN particles were homogeneously mixed

without any destruction in their morphology. Figure 7 depicts the high-magnification SEM image of individual SiC particles with a uniform coating of h-BN nanoparticles due to the adequate mixing of SiC/h-BN powders during ball-milling.

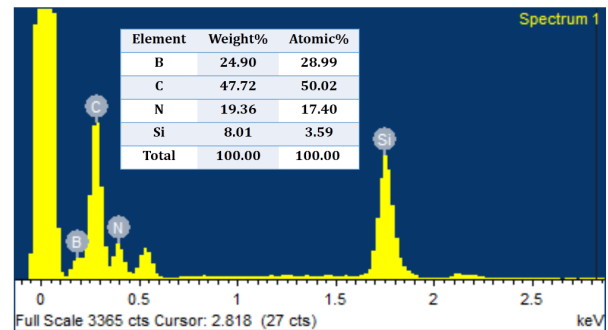
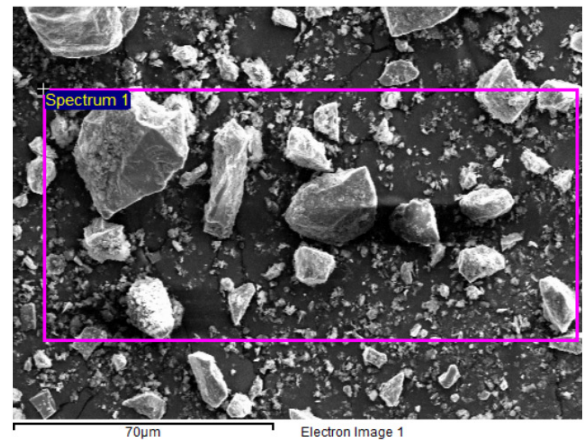


Figure 6 Low-magnification SEM image and EDS of the 4 h ball-milled SiC/h-BN powders.

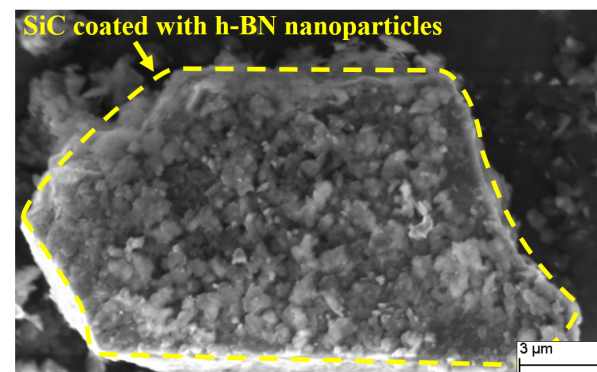


Figure 7. High-magnification SEM image 4 h ball-milled SiC/h-BN powders.

3.2 Microstructure analysis

The OM images of Al7075 and Al7075/SiC/h-BN HNC specimens are depicted in figures 8 (a-b). The micro and nano-size reinforcements are observed to be homogeneously distributed in the matrix owing to the combined approach of reinforcements pre-dispersion and ultrasonic-assisted melt stirring, as presented in figure 8b. The OM results show the variation in grain size (ultra-grain refinement) of prepared HNC compared to as-cast Al7075. This reduction in the grain size of the prepared HNC is mainly due to the reinforcement of micro and nano-size particles, thermal mismatch, reinforcement strengthening effect and ultrasonic-assisted melt stirring approach [20].

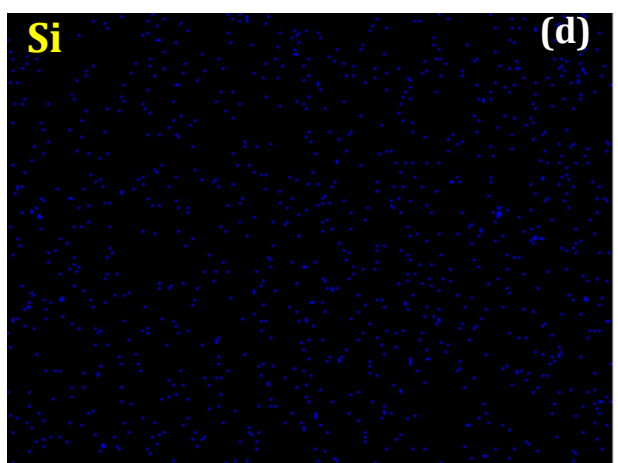
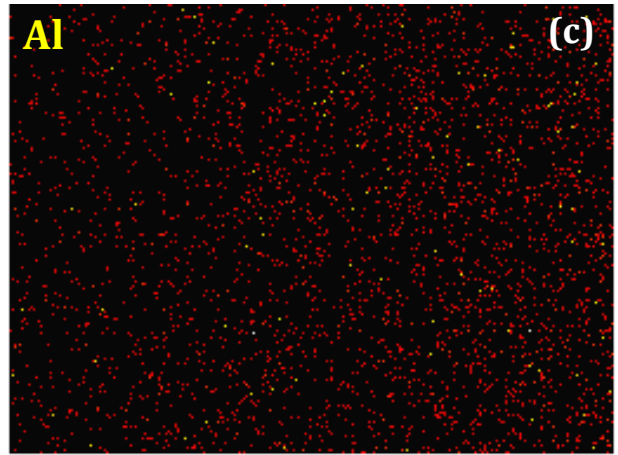
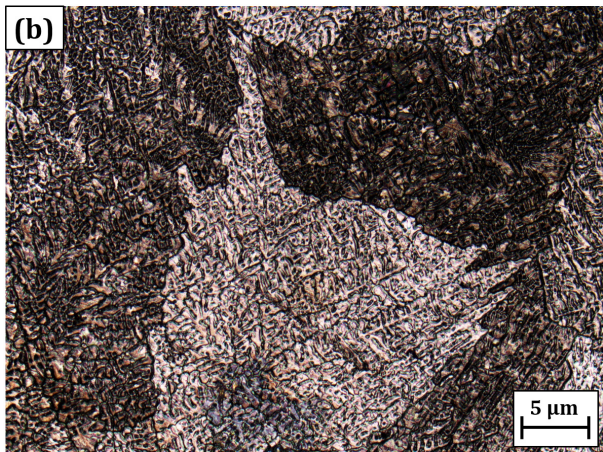
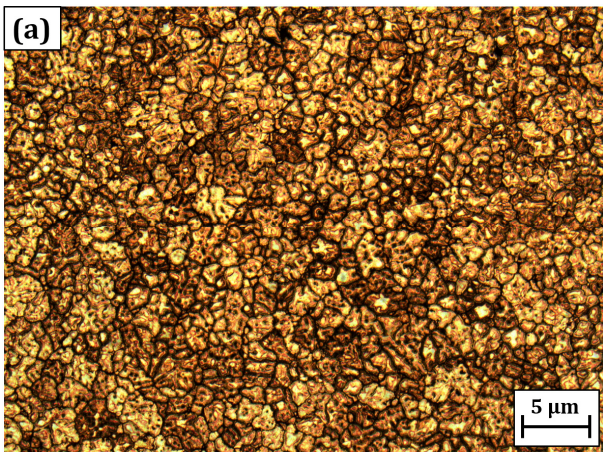


Figure 8. Optical micrographs of (a) Al7075 and (b) Al7075/SiC/h-BN hybrid nanocomposite specimens.

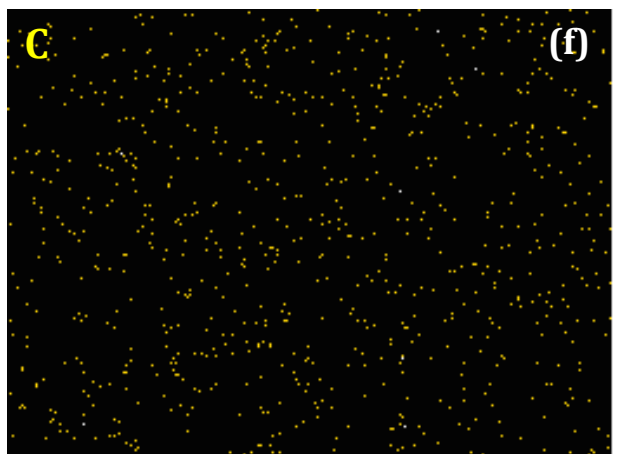
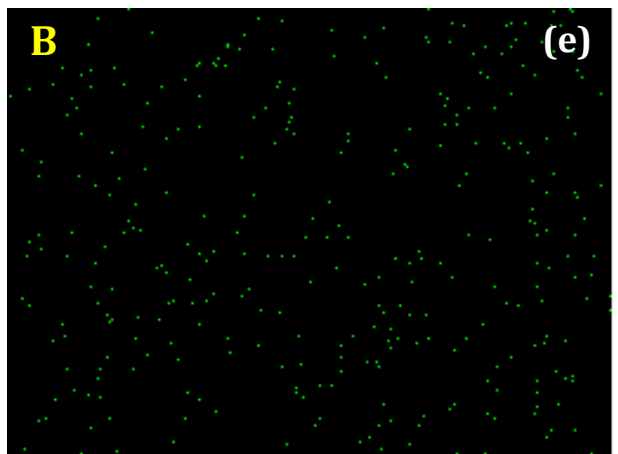
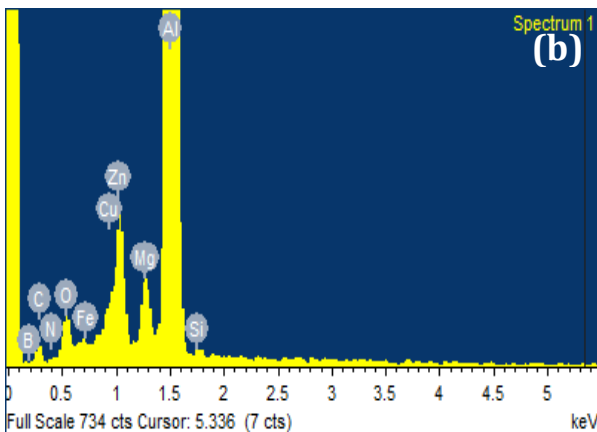
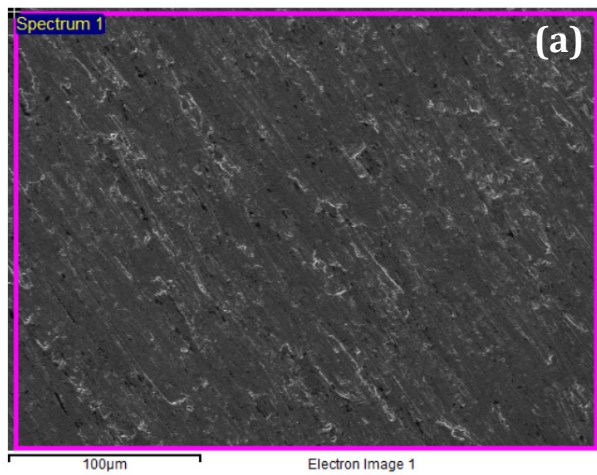




Figure 9. (a) SEM image, (b) EDS and (c-g) elemental mapping analysis of hybrid nanocomposite.

The SEM, EDS and elemental mapping analysis (SEM-MAP) of the fabricated HNC are presented in figure 9. From the EDS (figure 9b) and mapping analysis (figures 9c-g), the presence and uniform dispersal of reinforcements in the prepared HNC are observed.

3.3 Density and porosity

Densities (theoretical and experimental) and porosity percentage (%) of Al7075 and Al7075/SiC/h-BN HNC specimens are depicted in figure 10.

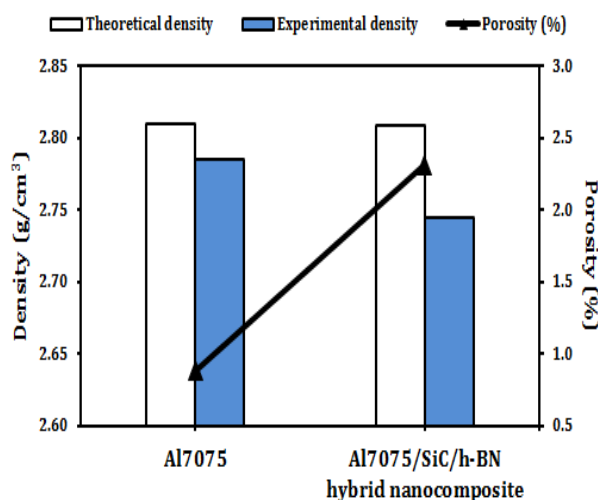


Figure 10. Density and % porosity of the prepared Al7075 and HNC specimens.

SiC and h-BN particles used in this investigation have density values of 3.22 g/cm³ and 2.27 g/cm³, respectively. The methodology adopted for evaluating the density and porosity % of the prepared specimens has been described elsewhere [13]. It was observed that the porosity (%) of HNC was higher than the unreinforced Al7075 specimen. The porosity of HNC is usually associated with clustering of reinforcements, the existence of air bubbles in the melt, poor wettability characteristics, shrinkage during solidification, nanoparticles agglomeration and gas entrapment during melt-stirring [20]. In this work, reinforcement pre-dispersion, optimized process parameters for squeeze casting [1] and ultrasonic-assisted mixing approach were adopted, to avoid the nanoparticle agglomeration, wettability issues and clustering of reinforcements.

3.4 Hardness

The average hardness (Rockwell) and microhardness (Vickers) of the Al7075 and Al7075/SiC/h-BN HNC specimens are shown in figure 11. The hardness of the HNC increases with the accumulation of SiC and h-BN particles in the Al7075 alloy matrix. The improvement of Vickers and Rockwell hardness for HNC is compared to Al7075 is 12.46% and 13.87%, respectively. The improvement in hardness can be owing to the combined influence of grains refinement and reinforcement strengthening effects [20]. Moreover, after squeeze casting when the prepared HNC is cooled to ambient atmosphere, the reinforcements used in the present work tend to strengthen the Al7075 matrix owing to their coefficient of thermal expansion (CTE) mismatch with the matrix.

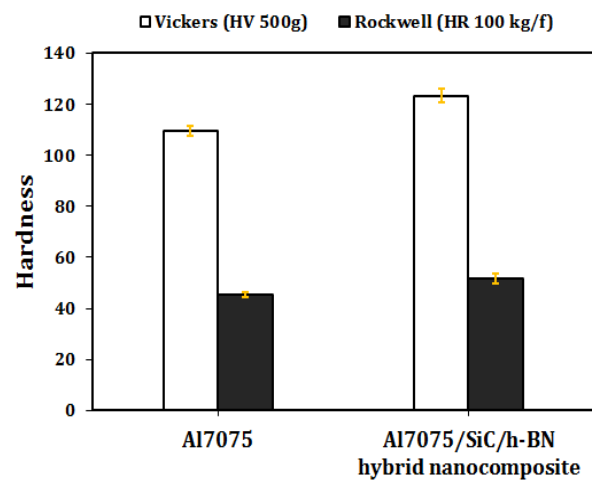


Figure 11. The hardness (Vickers and Rockwell) of the prepared Al7075 and HNC specimens.

3.5 UTS and YS

Figure 12 presents the variation of UTS and YS for squeeze-cast Al7075 and Al7075/SiC/h-BN HNC. From the obtained results, it is found that the YS increases by 35% for Al7075/SiC/h-BN HNC compared to the Al7075. Moreover, the augmentation of UTS for HNC compared to Al7075 is 21.69%. The improvement of YS and UTS of the fabricated Al7075/SiC/h-BN HNC is associated with grain refinement and strengthening effect of SiC and h-BN particles.

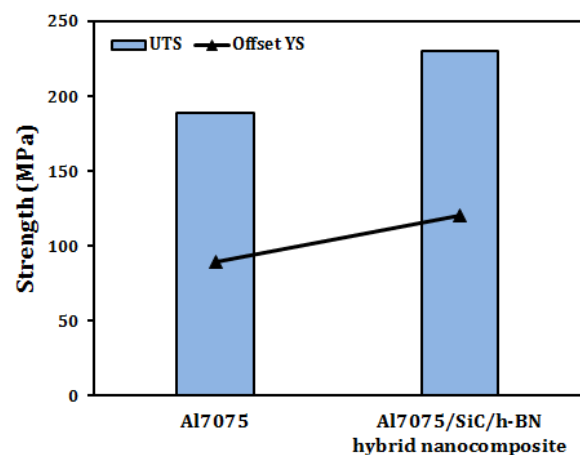


Figure 12. UTS and YS of the prepared Al7075 and HNC specimens.

3.6 Fracture surface microstructure analysis

Figures 13(a-b) depict the fracture surface microstructure of the Al7075/SiC/h-BN HNC specimen. The SEM image (figure 13a) illustrates the grain refinement, micro-cracks and tiny dimples. Moreover, the FE-SEM image (figure 13b) demonstrates fracture particles, ductile fracture of the Al7075 matrix and the presence of h-BN nanoparticles. The grain refinement is an indication of the strengthening of the HNC. The reinforcement of micro and nanoscale particles in the Al7075 matrix improved the load-bearing capacity of the resulting HNC.

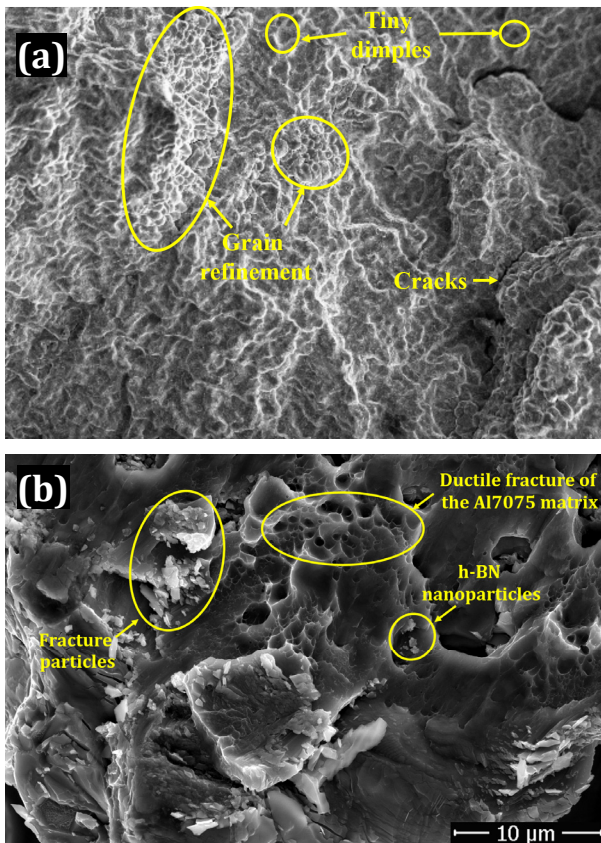


Figure 13. Fractured surface of Al7075/SiC/h-BN HNC specimen.

The mechanical properties of HNC are mainly influenced by different factors such as dispersion uniformity of reinforcements, matrix strength and interfacial bonding between the matrix and reinforcements. The findings described above divulge that the use of reinforcement pre-processing route and ultrasonic-assisted melt stirring helps to achieve the homogenous distribution of SiC and h-BN particles in the squeeze-cast HNC results in a substantial strength improvement. Moreover, it is also evident that the augmentation in the YS, UTS and hardness of the fabricated HNC is associated with grain refinement, reinforcement strengthening effects, thermal mismatch strengthening and dispersion uniformity of reinforced particles in the matrix [12–[14,20].

3.7 Cutting force and surface roughness

The cutting force generated during the machining operation of Al7075 and HNC specimens were recorded for different CS and FR at constant DOC. The effect of

CS and FR on the cutting force during the dry and MQL turning is illustrated in figures 14-15. The cutting force has been found to increase as the FR increases. Usually, the reinforcement of hard SiC particles in the matrix adds intricacy in the machining of resulting composites. However, in this study, the cutting force generated during the turning of Al7075/SiC/h-BN HNC is lesser as compared to the Al7075 specimen due to the reinforcement of h-BN nanoparticles. As compared to dry machining, in MQL machining, the lower cutting force was observed for both Al7075 and HNC specimens. The generation of less cutting force during the MQL machining operation of Al7075 and HNC specimens might be associated with the combined effect of cooling, lubrication and film-forming tendency of MQL. It is also observed that for both Al7075 and HNC specimens under dry and MQL machining environment, the cutting force decreases when the CS increases from 180 m/min to 200 m/min. An analogous trend has also been observed in the available literature [12], [16], [17].

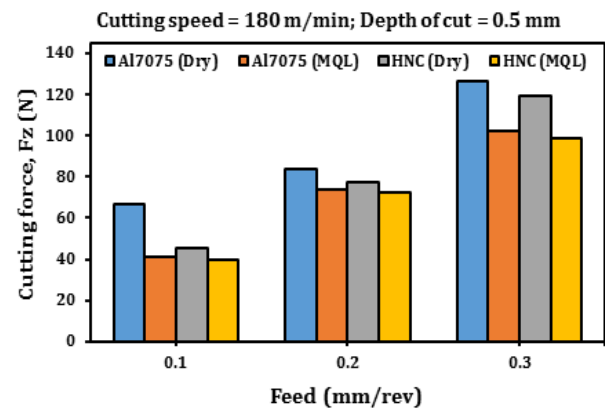


Figure 14. The effect of FR on cutting force at CS = 180 m/min and DOC = 0.5 mm under dry and MQL machining.

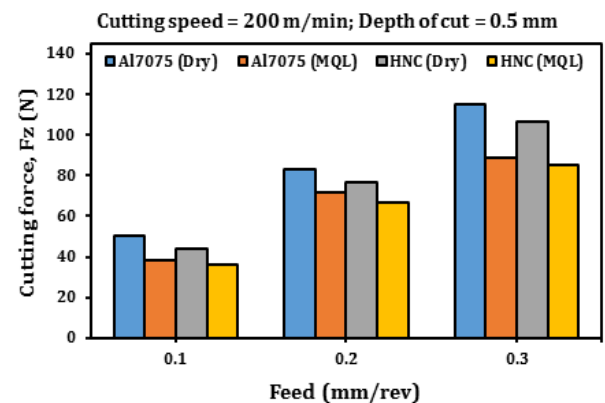



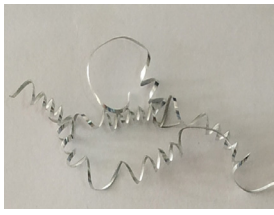

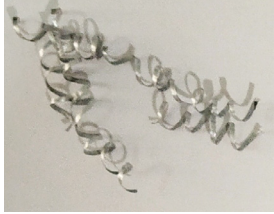












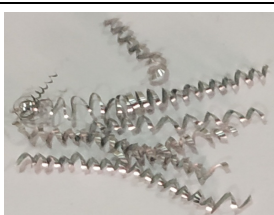
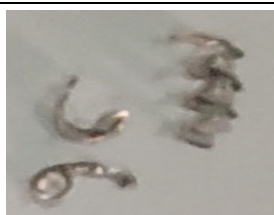





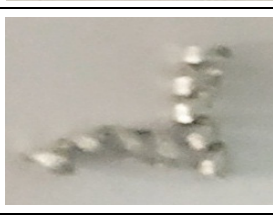
Figure 15. The effect of FR on cutting force at CS = 200 m/min and DOC = 0.5 mm under dry and MQL machining.

The effects of FR on the SR of Al7075 and HNC specimens are presented in figures 16 & 17. The formula used in the theoretical calculation of SR during the turning process is presented in equation 1 [12], [16].

$$SR \approx \frac{0.032f^2}{r_n} \quad (1)$$

SR – arithmetic mean value of surface roughness;
 f – feed rate;
 r_n – nose radius

Table 1. Chips length and morphology of squeeze-cast specimens under different machining environment.

Material ↓	Machining parameter and environment	Feed rates (at a constant DOC: 0.5 mm)		
		0.1	0.2	0.3
Aluminium 7075	CS: 180 m/min Machining environment: Dry			
	CS: 180 m/min Machining environment: MQL			
Al7075/SiC/h-BN hybrid nanocomposite	CS: 180 m/min Machining environment: Dry			
	CS: 180 m/min Machining environment: MQL			
Aluminium 7075	CS: 200 m/min Machining environment: Dry			
	CS: 200 m/min Machining environment: MQL			
Al7075/SiC/h-BN hybrid nanocomposite	CS: 200 m/min Machining environment: Dry			
	DOC: 0.5 mm CS: 200 m/min Machining environment: MQL			

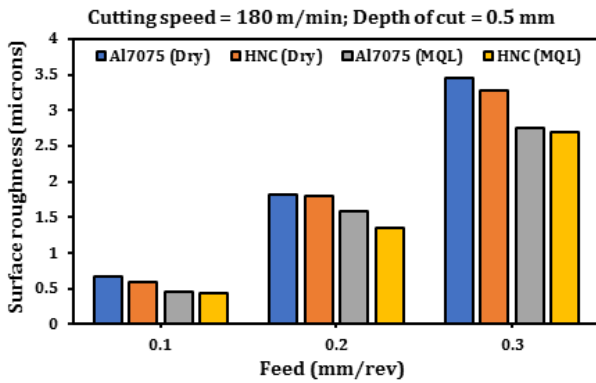


Figure 16. The effect of FR on SR of squeeze-cast Al7075 and HNC at CS = 180 m/min and DOC = 0.5 mm under dry and MQL machining.

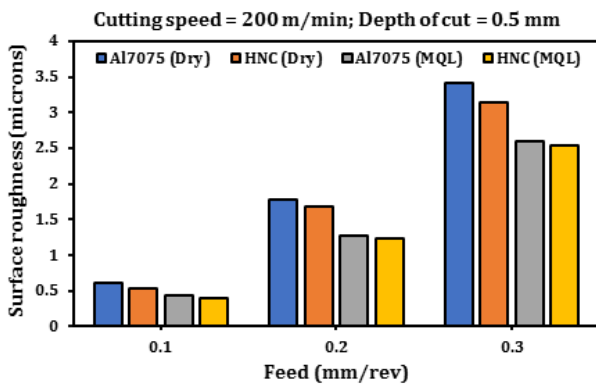


Figure 17. The effect of FR on SR of squeeze-cast Al7075 and HNC at CS = 200 m/min and DOC = 0.5 mm under dry and MQL machining.

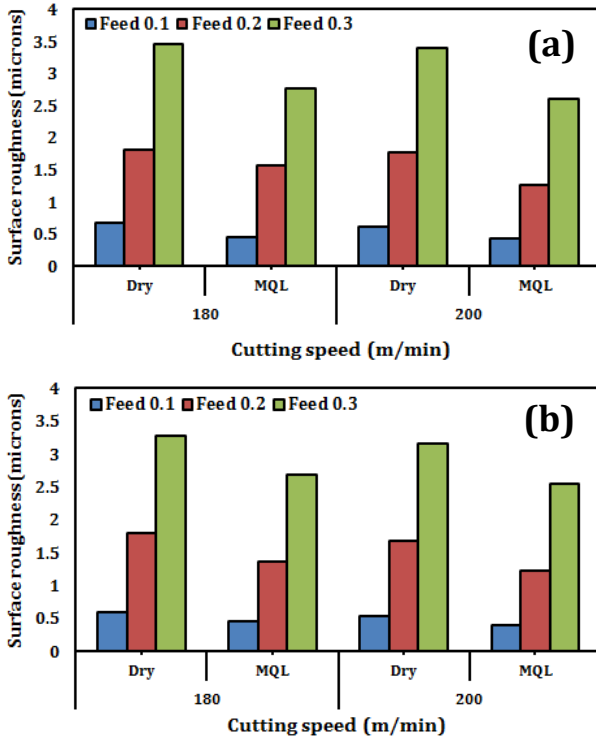


Figure 18. The effect of CS on SR of squeeze-cast (a) Al7075 and (b) HNC at FR = 0.1, 0.2, 0.3 mm and DOC = 0.5 mm under dry and MQL machining.

From equation 1, it is apparent that the SR increases with increasing FR. The analogous trend has also been found in the turning experiment of prepared Al7075 and HNC specimens. According to earlier literature, mate-

rial removal is augmenting in proportion with FR, which in turn enhances the temperature and cutting force. Further, this contributes to enhanced tool wear and consequently results in higher SR [14]. From figures 16-18, it is evident that the SR achieved during the MQL machining is less as compared to dry machining for both Al7075 and HNC specimens. The surface roughness was lower in HNC than the Al7075 specimens. This reduction was mainly owing to the presence of nanoscale h-BN particles in HNC specimens. The lowest SR was observed in the turning operation of HNC under the MQL machining conditions. This can be mainly due to the presence of an external thin lubricant layer provided by MQL and the establishment of a solid nano-lubricant layer achieved by reinforced h-BN nanoparticles. A similar trend has also been observed in the earlier literature.

3.8 Formation of chips

The chips of different length and morphology produced during the machining operation of Al7075 and Al7075/SiC/h-BN HNC specimens under dry and MQL environment are presented in table 1. The continuous chips were perceived during the dry turning of the Al7075 specimen. Though, in the HNC, the length of the continuous chip was significantly lower. This might be due to the generation of less cutting force during the turning operation of HNC. It is also found that the chip length observed during the MQL machining is less as compared to dry machining for both Al7075 and HNC specimens. Moreover, from table 1 it is evident that the chip length is decreasing with enhanced FR.

4. CONCLUSIONS

The Al7075 based hybrid nanocomposites reinforced with SiC and h-BN nanoparticles were successfully fabricated via ultrasonic-assisted squeeze casting method. The effect of SiC/h-BN reinforcements on the tensile strength, hardness, microhardness and microstructure of Al7075/SiC/h-BN hybrid nanocomposite was examined. Further, the machinability analysis has also been carried out to examine the effect of several machining parameters such as CS, FR and DOC on the machinability characteristics of the Al7075 and HNC specimens under dry and MQL machining conditions. The important findings drawn from the microstructural, mechanical and machining investigations are as follows:

1. It is found that the pre-dispersion technique (Ball milling) of reinforcing particles is a promising approach for achieving homogeneous mixing and dispersion of reinforcements in the resulting hybrid nanocomposite.
2. Mechanical characterization reveals that the trivial loading of SiC/h-BN particles in the Al7075 matrix considerably enhances the UTS, YS and hardness of the resulting HNC. This improvement is mainly due to binding among the reinforcements and matrix that do not allow it to deform easily.
3. The significant grain refinement was found in the Al7075/SiC/h-BN hybrid nanocomposite due to the implementation of an ultrasonic-assisted squeeze

casting approach and addition of hybrid reinforcements in the Al7075 matrix.

- The reinforced nanoscale h-BN particles acted as a solid lubricant during the dry turning operation and accommodated to attain the better surface quality of the machined surface.
- The lowest surface roughness and cutting force were observed during the MQL turning of HNC, which was associated with the combined lubrication layer mechanism achieved by reinforced h-BN nanoparticles and MQL.
- It is recommended to make the machining operation more economical and energy-efficient, the MQL machining is preferable compared to dry machining.

REFERENCES

- [1] A. Ramanathan, P. K. Krishnan, R. Muraliraja, "A review on the production of metal matrix composites through stir casting – Furnace design, properties, challenges, and research opportunities," *J. Manuf. Process.*, vol. 42, no. April, pp. 213–245, 2019.
- [2] K. Dey, J. R. Verlekar, S. K. Soni, and B. Thomas, "Dynamic analysis of functionally graded shaft," *FME Trans.*, vol. 47, no. 1, 2019.
- [3] C. M. L. Christopher, T. Sasikumar, C. Santulli, and C. Fragassa, "Neural network prediction of aluminum-silicon carbide tensile strength from acoustic emission rise angle data," *FME Trans.*, vol. 46, no. 2, pp. 253–258, 2018.
- [4] S.V. Alagarsamy and M. Ravichandran, "Synthesis, microstructure and properties of TiO₂ reinforced AA7075 matrix composites via stir casting route," *Mater. Res. Express*, vol. 6, no. 8, p. 086519, 2019.
- [5] V. Bharath, M. Nagaral, V. Auradi, and S. A. Kori, "Preparation of 6061Al-Al₂O₃ MMC's by Stir Casting and Evaluation of Mechanical and Wear Properties," *Procedia Mater. Sci.*, vol. 6, no. Icmpe, pp. 1658–1667, 2014.
- [6] R. Surendran, N. Manibharathi, and A. Kumaravel, "Wear properties enhancement of aluminium alloy with addition of nano alumina," *FME Trans.*, vol. 45, no. 1, pp. 83–88, 2017.
- [7] S. Venkatesan and M. Anthony Xavier, "Tensile behavior of aluminum alloy (AA7050) metal matrix composite reinforced with graphene fabricated by stir and squeeze cast processes," *Sci. Technol. Mater.*, vol. 30, no. 2, pp. 74–85, 2018.
- [8] M. Ramesh, J. D. Daniel, M. Ravichandran, "Investigation on Mechanical Properties and Wear Behaviour of Titanium Diboride Reinforced Composites," *FME Trans.*, vol. 47, pp. 873–879, 2019.
- [9] M. Nagaral, R. Pavan, P. S. Shilpa, and V. Auradi, "Tensile Behavior of B₄C Particulate Reinforced Al2024 Alloy Metal Matrix Composites," *FME Trans.*, vol. 45, no. 1, pp. 93–96, 2017.
- [10] P. S. Samuel Ratna Kumar, D. S. Robinson Smart, and S. John Alexis, "Corrosion behaviour of Aluminium Metal Matrix reinforced with Multi-wall Carbon Nanotube," *J. Asian Ceram. Soc.*, vol. 5, no. 1, pp. 71–75, 2017.
- [11] P. Ashwath, M. Anthony Xavier, "Effect of microwave heat treating processing on frictional behaviour of aluminium alloy 2900 composites," *Tribol. - Mater. Surfaces Interfaces*, vol. 5831, pp. 1–12, 2018.
- [12] P. Agarwal, A. Kishore, V. Kumar, S. K. Soni, and B. Thomas, "Fabrication and machinability analysis of squeeze cast Al 7075/ h-BN/graphene hybrid nanocomposite," *Eng. Res. Express*, vol. 1, no. 1, p. 015004, 2019.
- [13] S. K. Soni and B. Thomas, "Influence of TiO₂ and MWCNT nanoparticles dispersion on microstructure and mechanical properties of Al6061 matrix hybrid nanocomposites," *Mater. Res. Express*, vol. 6, no. 12, p. 1265f3, 2020.
- [14] A. P. Reddy, et al.: "Strengthening and Mechanical Properties of SiC and Graphite Reinforced Al6061 Hybrid Nanocomposites Processed Through Ultrasonically Assisted Casting Technique," *Trans. Indian Inst. Met.*, vol. 72, no. 9, pp. 2533–2546, 2019.
- [15] M. Elango, K. Annamalai, "Machining Parameter Optimization of Al / SiC / Gr Hybrid Metal Matrix Composites using ANOVA and Grey Relational Analysis," *FME Trans.*, vol. 48, pp. 173–179, 2020.
- [16] C. Kannan, R. Ramanujam, and A. S. S. Balan, "Machinability studies on Al 7075/BN/Al₂O₃ squeeze cast hybrid nanocomposite under different machining environments," *Mater. Manuf. Process.*, vol. 33, no. 5, pp. 587–595, 2018.
- [17] A. Kumar, M. M. Mahapatra, and P. K. Jha, "Effect of machining parameters on cutting force and surface roughness of in situ Al–4.5%Cu/TiC metal matrix composites," *Measurement*, vol. 48, no. 1, pp. 325–332, 2014.
- [18] J. P. Ajithkumar and M. A. Xavier, "Flank and crater wear analysis during turning of Al 7075 based hybrid composites," *Mater. Res. Express*, vol. 6, no. 086560, 2019.
- [19] S. K. Soni and B. Thomas, "A comparative study of electrochemical machining process parameters by using GA and Taguchi method," *IOP Conf. Ser. Mater. Sci. Eng.*, vol. 263, no. 6, p. 062038, 2017.
- [20] C. Kannan and R. Ramanujam, "Comparative study on the mechanical and microstructural characterisation of AA 7075 nano and hybrid nanocomposites produced by stir and squeeze casting," *J. Adv. Res.*, vol. 8, no. 4, pp. 309–319, 2017.

**ИСТРАЖИВАЊЕ МИКРОСТРУКТУРЕ,
МЕХАНИЧКИХ СВОЈСТАВА И ОБРАД-
ЉИВОСТИ ХИБРИДНОГ НАНОКОМПОЗИТА
НА БАЗИ А17075/SiC/h И ВН ПРОИЗВЕДЕНОГ
ЛИВЕЊЕМ ИСТИСКИВАЊЕМ УЗ ПОМОЋ
УЛТРАЗВУКА**

С.К. Сони, Б. Томас

Рад се бави истраживањем микроструктуре, механичких својстава и обрадљивости хибридног наноконтрола од А17075 и А17075/SiC/h-BN добијеног

ливењем истискивањем. Легура нанокompозита Al7075 је ојачана честицама SiC (1 wt%) микро-димензија и наночестицама h-BN (0,5 wt %) које су припремљене мешањем растопине уз помоћ ултразвука. Да би се постигло боље мешање ојачања, смањено ефекат агломерације наночестица и боља кваљивост у растопини, SiC и h-BN у прашкастом стању су подвргнути обради куглицама у трајању од 4 часа. Истраживање микроструктуре припремљеног нанокompозита је обављено коришћењем OM, SEM и анализом мапирања рендген зрака. Мапирање и OM метода показују добру дистрибуцију ојачања и

пречишћеност димензија честица. Истраживање механичких својстава показује значајно побољшање (35,33%; 21,69%; 13,87%; 12,27%) вредности напона развлачења, затезне чврстоће, тврдоће по Роквелу, односно микротврдоће (Викерс). Анализа обрадљивости је обављена да би се испитао утицај неколико параметара обраде као што је брзина резања, брзина помоћног кретања и дубина резања на храпавој површини, силу резања и дужину струготине у условима сувог и минималног подмазивања при обради. Резултати анализе обрадљивости су упоређени са узорком Al7075 и потом размотрени.